Available online at www.sciencedirect.com

SciVerse ScienceDirect

Energy Procedia 24 (2012) 176 – 185

Energy Procedia

DeepWind, 19-20 January 2012, Trondheim, Norway

First results of turbulence measurements in a wind park with the Small Unmanned Meteorological Observer SUMO

Joachim Reuder and Marius O. Jonassen

Geophysical Institute, University of Bergen, Allegaten 70, N-5007 Bergen, Norway

Abstract

The Small Unmanned Meteorological Observer (SUMO), equipped with a miniaturized 5-hole probe for turbulent flow measurements with 100 Hz temporal resolution, has for the first time been operated in and around a wind farm. The 5 day campaign from May 9-13 took place at a small wind park of 21 1 MW-turbines close to Vindeby on Lolland, Denmark and was dedicated to the investigation of the effects of wind turbines on boundary layer turbulence.

A total of 20 SUMO flight missions carrying the turbulence system have been performed during the campaign. In spite of a few pitfalls related to the fine-tuning of the autopilot system and in the configuration and synchronization of the corresponding data logging systems, this campaign provided promising results indicating the capability and future potential of small UAS for turbulence characterization in and around wind farms. Subsequent flights upwind and downwind of the park revealed qualitatively a distinct enhancement in the turbulence level behind the wind farm.

Keywords: atmospheric boundary layer (ABL); turbulence; wind park; wind energy; unmanned aircraft system (UAS);

1. Introduction

Atmospheric turbulence is one of the key parameters in wind turbine operation. The understanding of turbulence induced by individual wind turbines is crucial for the layout and operation of wind farms, as it leads to production losses and an increase in loads and fatigue. The structure and intensity of turbulence created by a wind farm will, in combination with atmospheric stability, also determine the potential of recovery of surface layer winds by downward mixing of momentum from the atmospheric boundary layer

 doi:10.1016/j.egypro.2012.06.099

above. This is an important factor for siting and spacing of larger offshore arrays of turbines planned during the next years.

Direct turbulence measurements in the atmospheric boundary layer are up to now mainly performed by sonic anemometers at fixed masts or by low-level flights of manned aircraft equipped with directional flow sensors (e.g. [1], [2]). Both measurement methods comprise certain serious drawbacks for applications around single wind turbines or in and around wind farms. The first one is rather inflexible and infrastructural demanding, the second one is very costly and highly restricted with respect to proximity of measurements to the turbines or wind park by safety considerations.

During the last years, unmanned aircraft systems (UAS) have significantly extended the measurement capabilities in Atmospheric Boundary Layer (ABL) research, providing cost-efficient and flexible sensor platforms for the characterization of the ABL with reasonably high temporal and spatial resolution (e.g. [3-5]). Such measurement systems have also an extraordinary potential to increase our understanding of turbulence and wake effects, both of single wind turbines and of wind farms [6,7]. In particular, very small and lightweight (< 1 kg) systems will be of relevance for this purpose, as they do not represent a serious threat for the wind turbines in case of a collision.

With the Small Unmanned Meteorological Observer (SUMO), a corresponding platform has been developed during the last 5 years [5], performing more than 700 scientific flight missions in the ABL since 2007. Up to now, the system has mainly been operated as controllable and recoverable sounding system for the measurement of temperature, humidity and wind profiles from the ground up to more than 3000 m. The collected data have been the basis for ABL process studies and model validation [8,9]. The system is currently under development towards full measurement capability for the turbulent wind vector in the atmosphere, which is the main topic of the present study.

Section 2 will shortly present the SUMO system and its instrumentation and Section 3 gives an overview over the measurement campaign. Section 4 describes the experiences with the advanced instrumentation and presents exemplary results from two different flight patterns, before summarizing and presenting an outlook on future potential for improvement in Section 5.

2. The SUMO system

SUMO is based on the commercially available model construction kit FunJet by Multiplex, a delta-wing airframe composed from EPP foam material. With its wingspan and length of around 80 cm and a total take-off weight of around 600 g it falls into the category of micro-UAS. The aircraft has electric propulsion by a 120 W brushless motor driving a pusher-propeller in the rear. SUMO has been developed in cooperation between the Geophysical Institute, University of Bergen, Norway and Martin Müller Engineering, Hildesheim, Germany. A detailed description of the system can be found in Reuder et al. [5]. Fig. 1 shows one of the 3 SUMO systems operated during the campaign, the key technical specifications are summarized in Table 1.

SUMO is equipped with the open source autopilot system Paparazzi, mainly developed and maintained by the École Nationale de l'Aviation Civile (ENAC), Toulouse, France. This freely available autopilot software and hardware package is used by several hundreds of educational and scientific users all over the world. It enables the aircraft to be flown autonomously under the supervision of an experienced RC pilot and a ground control station (GCS) operator. The system enables automatic flights following predefined mission plans that can be modified at any time in-flight using the 2.4 GHz bidirectional data link. For attitude monitoring and control, the miniaturized IMU (inertial measurement unit) ArduIMU from Diydrones is used.

In its current version, the SUMO system is equipped with the following sensors for basic meteorological parameters. Temperature and humidity are measured by the combined sensor SHT 25 from

Sensirion. This sensor is mounted inside a radiation protection tube on the upper side of the wing (see Fig. 1). Atmospheric pressure is monitored by a SCP1000 sensor from VTI inside the fuselage. The surface temperature below the aircraft can be estimated with the help of an IR sensor (MLX90247).

Table 1. Technical specifications of the SUMO system

vehicle type	fixed wing UAS
DIMENSIONS	
Wingspan	0.80 m
Length	0.75 m
Height	0.23 m
propeller diameter	227 mm (9”x6”)
take-off weight	600 g
PROPULSION	
Motor	electric brushless
motor type	AXI2212/26
motor power	120 W
battery type	lithium-polymer (3 cells)
battery capacity	2.4 Ah/11.1 V
SPEED AND ENDURANCE	
minimum speed	8 m/s
maximum speed	42 m/s
cruise speed	15 m/s
horizontal range	< 10 km
vertical range	> 4 km
flight duration	< 40 min

For flow measurements the SUMO system has been equipped with 2 different sensors. The first one is a rather simple and inexpensive Pitot tube (Airspeed Sensor v3 from Eagle Tree Systems), typically used for air speed measurements by model aircraft enthusiasts. This sensor has been directly connected to the data system of the Paparazzi autopilot and configured for a maximum measurement rate of around 7 Hz. As the preliminary results of this sensor look not very promising from a scientific point of view, this data set is not further investigated in this study. The second flow measurement system consists of a miniaturized a 5-hole probe and the corresponding pressure transducers and data logger, commercially available from Aeroprobe Corporation in the USA. The system is capable to measure the 3-dimensional turbulence flow vector impinging the aircraft with a temporal resolution of 100 Hz. The mounting of the

5-hole probe is shown in Fig. 1. The technical details and characteristics of the adapted sensors are summarized in Tab. 2.

Fig. 1. Mounting of the turbulence system on the SUMO aircraft.

Table 2. Specifications of the meteorological sensors currently carried by the SUMO airframe

parameter	sensor	range	accuracy	acquisition frequency
temperature	Sensirion SHT 75	-40/+124 °C	+/-0.3 K	2 Hz
relative humidity	Sensirion SHT 75	0-100 %	+/-2 %	2 Hz
pressure	VTI SCP1000	300-1200 hPa	+/-1.5 hPa	2 Hz
surface temperature	MLX90247	n/a	n/a	2 Hz
3 D flow vector	5 hole probe, Aeroprobe	11-35 m/s	0.1 m/s	100 Hz
1 D flow vector	Pitot tube, Eagle Tree	1-156 m/s	n/a	7 Hz

During the deployments in the flight week, the data logger of the turbulence probe had to be operated stand-alone without synchronization with the autopilot continuously logging the attitude of the aircraft, i.e., the Eulerian angles pitch, roll and yaw. These are essential to apply the correction for the movement of the aircraft to transform the in-flight measured turbulent flow into the meteorologically relevant components u (east-west), v (north-south), and w (in the vertical). Due to limitations in the bandwidth of the data transmission between SUMO and the GCS and a lack of corresponding on-board storage capacity, the attitude information during the turbulence flights has in addition been limited to 10 Hz sampling rate. For the turbulence flight missions performed during the flight week at Nøjsomhed, this leaves us with the

challenging task of motion correction based on two unsynchronized data sets with different temporal resolution.

3. Campaign

A 5 day measurement campaign was performed in the period May 9 to 13, 2011 at the Nøjsomheds Odde wind farm near Vindeby, on the island of Lolland, Denmark. The wind park is operated by DONG Energy and consists of 21 turbines with a nominal power output of 1 MW (Bonus 1000). The turbines have a hub height of 55 m and a rotor diameter of 52 m. The field experiment was an integral part of the joint research project "Autonomous Aerial Sensors for Wind Power Meteorology" funded by Energinet.dk and supported by the International Wind Academy Lolland, IWAL.

A laser wind profiler (ZephIR from Narural Power) was continuously operated during the campaign at the Northeastern corner of the wind farm by DTU Risø. In addition, DTU Risø and the company Delta tested a sonic turbulence probe mounted below a LTA (Lighter-than-Air) system from Skydoc.

The SUMO system performed a total of 71 flight missions during the campaign, 20 of them carrying the newly adapted 5-hole turbulence probe. The applied flight patterns were longer horizontal transects of around 1 km in length (e.g. those presented in Fig. 3) and race track patterns around groups of turbines, e.g the three eastern ones as shown in Fig. 4.

4. Results

The left panel of Fig. 2 shows an example of such a race track pattern. The turbines of the park are denoted as red triangles, the projection of the flight path is given by the white line. Marked in green and red are the straight portions of the flight path selected for the statistical analysis of the turbulence data.

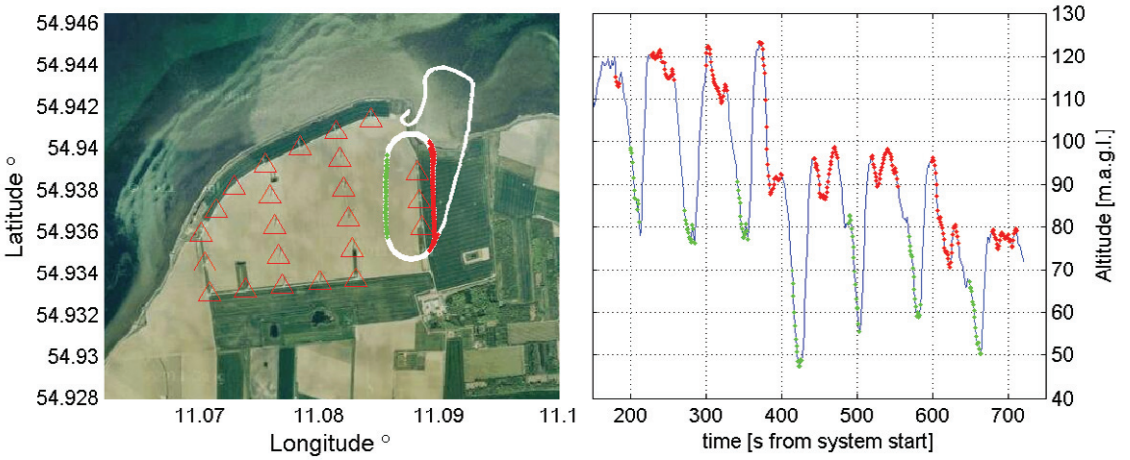

Fig. 2. Race-track pattern flown with the turbulence probe in the Nøjsomhed wind farm (left) on 12.05.2011, 12:09 UTC, and the corresponding time series of the altitude of the SUMO aircraft. The positions of the turbines are indicated with the red triangles. The red and green markers indicate the straight parts of the flight pattern used for further turbulence investigations. The pattern was flown clockwise, the wind coming from SW, i.e. SUMO senses headwind component on the eastern part of the track (red) and tailwind on the western part (green). (Google-bilder © 2011 COWI A/S, DDO, DigitalGlobe, GeoEye, Scankort © Google)

During the flight, the wind was blowing from SSW with around 6 m/s. Flying the pattern in clockwise direction this leads to a tailwind component on the western part of the track (green) and headwind on the eastern part (red).

The right panel in Fig.2 shows the corresponding time series of the aircraft's altitude. The straight sections of the flight path are again identified by the color code. The nominal flight levels prescribed to the autopilot were 100 m (150 s-350 s), 75 m (400 s-600 s) and 55 m (> 600 s). In average, this value is valid, but during each round on the racetrack the altitude shows an oscillation with an amplitude of around 20 m. The altitude regulation by the autopilot works in this case much better, but is far from optimal, for the headwind conditions, while the aircraft loses altitude nearly continuously in tailwind on the straight westward legs. This unsatisfactory behavior of the SUMO aircraft in keeping the predefined altitude was caused by non-optimal fine tuning of the newly integrated IMU during the flight week. This issue was reworked after the campaign and the operation of SUMO during a follow up campaign in June/July 2011 in France showed excellent leveling characteristics, with typical altitude variations below 3 m for arbitrary flight patterns, even in strong wind conditions.

Fig. 3 shows exemplary the measured time series of the vertical component of the wind vector with a temporal resolution of 100 Hz. The shaded areas indicate the intervals where the SUMO was flying on the straight legs. The red and green dots and bars indicate the corresponding averages and standard deviations for each leg. The average values of the vertical component in the coordinate system of the aircraft are higher for the headwind legs which can be explained by a change of the average pitch angle of SUMO from headwind (nose up) to tailwind (nose down). A more detailed analysis of the data of this particular flight pattern seems not to be feasible due to the instability of the altitude regulation by the autopilot discussed above.

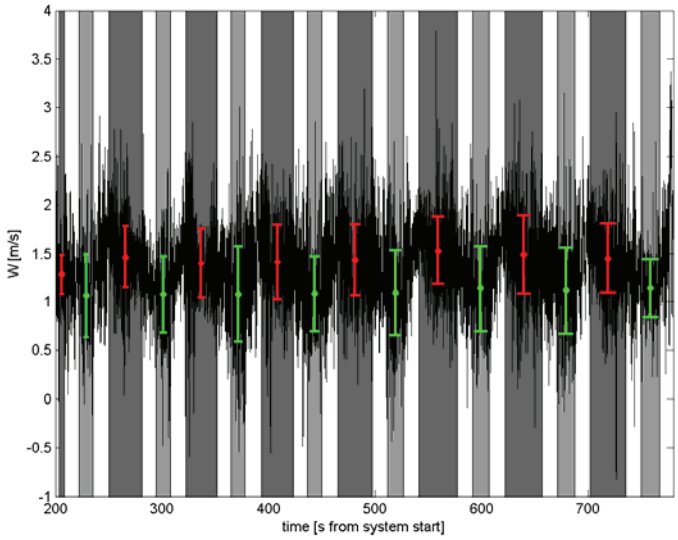

Fig. 3. Time series (100 Hz) of the vertical flow component (w) in the aircrafts coordinate system. The grey shaded areas mark the straight parts of the flight legs as also given in Fig. 2. The colored dots and bars indicate the average and standard deviation for each of those straight legs.

The following example is based on two flights performed on 12.05.2011 at 13:51 UTC and 14:37 UTC. The flight missions were designed to give an indication on the effect of the wind park on the turbulence structure of the ABL. For this flight with its longer legs terminated by turning circles, the altitude regulation of the autopilot was working much better than in the case described above. The wind at that time was blowing from WSW with wind speeds of around 5 m/s. The projection of the two flights is shown in Fig. 3. The western flight path (green), was slightly offshore and parallel to the coastline, and can be considered to represent the undisturbed marine boundary layer. In contrast, the eastern track (cyan) can be expected to be heavily affected by turbulence induced by the 21 wind turbines. Both missions have been performed at an altitude of 80 m and the straight leg has been repeated 4 times to improve the statistics.

In a first step the power spectra of the uncorrected raw data have been investigated for a basic analysis of the capability of the turbulence system in resolving atmospheric turbulence. As an example the time series of one of the straight flight legs (SW-NE direction, green trajectory in Fig 4) of around 750 m length, corresponding to approximately 30 seconds or 3000 data points of 100 Hz resolution, has been spectrally analyzed. The results of this analysis are shown in Fig. 5 for the cross-wind component v and the vertical component w. The two power spectra follow in general the expected -5/3 slope corresponding to the inertial subrange of a Kolmogorov spectrum for frequencies above 2 Hz. That behavior indicates that the system is capable of resolving atmospheric turbulence in this part of the frequency spectrum. The excess energy visible in the spectrum of v between 1 and 2 Hz is most likely correlated to a time constant of the yaw control loop of the autopilot system. The slight enhancement of the energy spectrum at frequencies above 30 Hz, most easily detectable in the v spectrum, but also visible in the w spectrum, could be related to aliasing effects caused by the basic update frequency of the autopilot of 60 Hz. A detailed analysis and interpretation of these spectra has to wait until motion corrected 100 Hz data sets are available with an improved version of the SUMO system in the future.

Fig. 4. The flight patterns for two missions on 12.05.2011. During these flights the wind was blowing from WSW with a speed of around 5 m/s. The western flight path (green) thus represents undisturbed offshore inflow conditions, while the eastern path (cyan) is expected to be significantly affected by the wind farm. The red red triangles indicate the positions of the wind mills in the park. (Google-bilder © 2011 COWI A/S, DDO, DigitalGlobe, GeoEye, Scankort © Google)

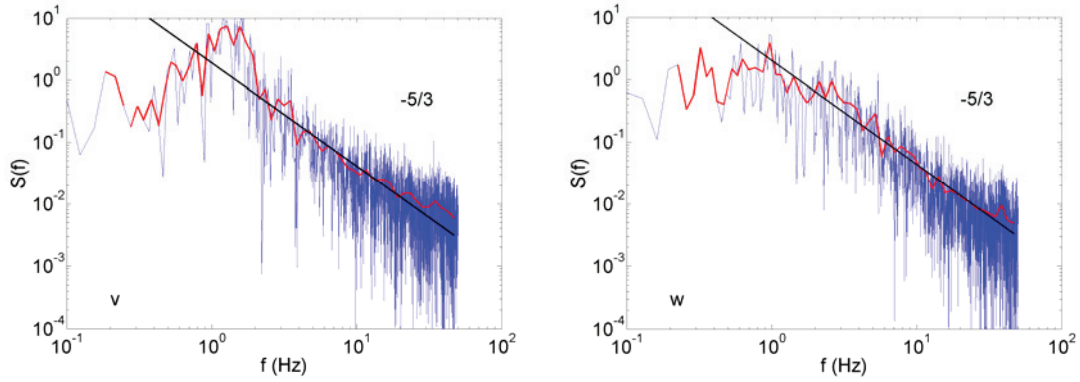

Fig. 5. Power spectra of the raw data in crosswind direction of the aircraft's main axis (v, left panel) and in the vertical (w, right panel) of the 5-hole probe turbulence system. The raw spectrum is given in blue, an averaged version in red. The black line corresponds to the theoretical -5/3 dependency of the inertial subrange of a Kolmogorov spectrum.

Fig. 6 presents the turbulent wind components in the aircraft's coordinate system. The left panels show the data for the undisturbed offshore flow conditions approaching the wind park (green flight path in Fig. 4), the right panels represent the turbulence mainly induced by the presence of the wind turbines. The grey bands in the panels indicate the time intervals where the aircraft was on a stable straight flight path at a certain distance from the turns. Again the standard deviation is expressed by the length of the red bar for each leg. Already the purely visual inspection of the raw data reveals distinct differences in the flow and turbulence structure in front of and behind the wind turbines. All components show a largely increased temporal variability downstream of the wind park. The continuous decrease visible in the u component of the flow vector, in particular visible in the undisturbed case (upper left panel in Fig. 6), is a result of the decreasing battery voltage and corresponding loss in motor power with time.

The results clearly show that the turbulence intensity is increased by around a factor of 3 behind the wind turbines compared to the undisturbed level of the incoming marine boundary layer flow. There is also a clear indication of an increase in the vertical velocity downwind of the park, potentially indicating lifting of part of the incoming air. These preliminary findings have of course to be validated and endorsed by the evaluation of all the SUMO flights performed during the campaign. It has to be taken into account that part of the increase in turbulence and of the vertical velocity change could also be explained by other processes, e.g. the build-up of an internal boundary layer over land caused by a change in surface roughness and/or surface heat fluxes due to insolation and strong heating of the ground, leading to local convective activity of increasing depth.

In general the achieved results are nevertheless very promising and encouraging. They give a strong indication for the capability and future potential of small UAS for turbulence characterization in and around wind farms. A more quantitative evaluation of the turbulence data requires the application of a correction algorithm for the aircraft's movement. As described in Section 2, this is a challenge due to synchronization and time resolution issues of the autopilot's data acquisition system in its current state. A corresponding upgrade of the SUMO system is ongoing and expected to resolve these issues within the next few months.

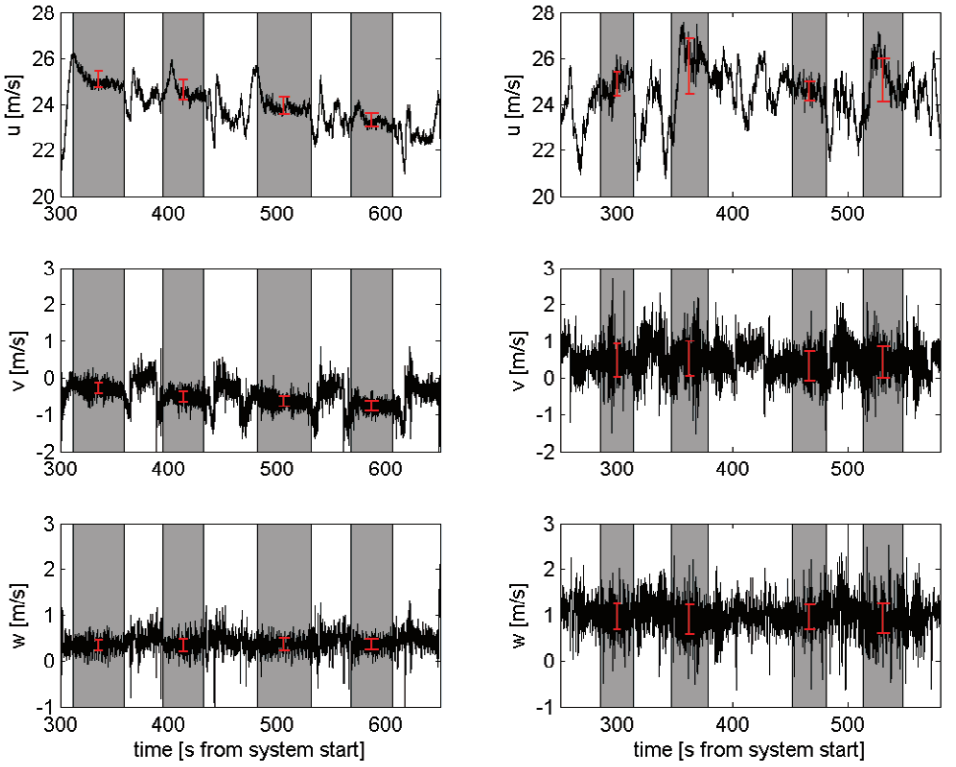

Fig. 6. Turbulent wind components in the aircraft coordinate system (not corrected for aircraft movement and attitude) measured with a frequency of 100 Hz. The left hand side represents the undisturbed, incoming offshore flow (green pattern in Fig. 4),the right hand side the boundary layer flow after being affected by the wind farm (blue pattern in Fig. 4).

5. Summary and Conclusions

The application of SUMO during a 5 day campaign in and around Nøjsomheds Odde wind farm in Denmark has clearly shown the capability of the system for measurements of atmospheric flow and turbulence in the vicinity of wind turbines. The preliminary results indicate a distinct increase in the turbulence intensity downstream together with evidence of enhanced mean vertical velocity. The main pitfall in atmospheric turbulence determination was the lack of a common data acquisition system for the turbulent flow vector impinging the aircraft and the attitude of the airframe. Therefore a more detailed investigation has to be postponed. The synchronization of the data acquisition of the 5-hole turbulence probe and the Paparazzi autopilot system is currently ongoing. From the beginning of 2012 both data streams will be commonly collected and stored on-board using the same temporal resolution of 100 Hz.

One reason for the increased standard deviation in all 3 flow components is for sure the increased turbulence intensity behind the wind park. However part of the observed difference could also be

addressed to general differences in the flight behavior of the SUMO aircraft under varying conditions. The upstream measurements have been done in a flight pattern nearly parallel to the mean wind direction, therefore operating SUMO either with head or tailwind, while the flight path behind the turbines is characterized by a large crosswind component. As it is not fully clear how this has affected SUMOs flight characteristics, the data presented here should be interpreted with care. Uncertainties of this kind will hopefully be removed in the future, as soon as the new data acquisition system allowing for the accurate correction of aircraft movement, currently under development, will be available. In addition could the build-up of an internal boundary layer over land due to corresponding changes in surface roughness or surface heat flux have affected the measurements.

Acknowledgements

The research work presented in this study was supported by the ForskEL project "Autonomous Aerial Sensors for Wind Power Meteorology (project number 10268). The authors are grateful to Martin Müller and Christian Lindenberg for developments on the SUMO system and for acting as ground control station operator and safety pilots during the field campaign. Many thanks also to Jesper Hjelme from IWAL (International Wind Academy Lolland) for his invaluable help and assistance during the field experiment.

References

[1] Stull RB. *An Introduction to Boundary Layer Meteorology.* Dordrecht: Kluwer Academic Publishing; 1988.

[2] Foken T. *Micrometeorology.* Berlin: Springer; 2008.

[3] Holland GJ, Webster PJ, Curry JA, Tyrell G, Gauntlett D, Brett G, et al.. The Aerosonde robotic aircraft: A new paradigm for environmental observations, *Bull Am Met Soc 2001;* **82**:889-901.

[4] Spiess T, Bange J, Buschmann M, Vörsmann P. First application of the meteorological Mini-UAV M^2AV. *Meteorol Z* 2007; **16**:159–69.

[5] Reuder J, Brisset P, Jonassen M, Müller M, Mayer S. The Small Unmanned Meteorological Observer SUMO: A new tool for atmospheric boundary layer research. *Meteorol Z* 2009;18:141-7.

[6] van den Kroonenberg A, Martin S, Beyrich F, Bange J. Spatially-Averaged Temperature Structure Parameter Over a Heterogeneous Surface Measured by an Unmanned Aerial Vehicle. *Boundary-Layer Meteorol* 2011;DOI 10.1007/s10546-011-9662-9.

[7] van den Kroonenberg A, Martin T, Buschmann M, Bange J, Vörsmann P. Measuring the Wind Vector Using the Autonomous Mini Aerial Vehicle M^2AV. *J Atmos Oceanic Technol*; **25**: 1969-81.

[8] Reuder J, Ablinger M, Ágústsson H, Brisset P, Brynjolfsson B, Garhammer M, et al. FLOHOF 2007: An overview of the mesoscale meteorological field campaign at Hofsjökull, Central Iceland. *Meteorol Atmos Phys* 2011;DOI10.1007/s00703-010-0118-4.

[9] Mayer S, Sandvik A, Jonassen M, Reuder J. Atmospheric profiling with the UAS SUMO: a new perspective for the evaluation of fine-scale atmospheric models. *Meteorol Atmos Phys* 2010;DOI10.1007/s00703-010-0063-2.